



Geological and Geochemical Characterization of Kyanite-Bearing Rocks Around Kuta Part of Minna Sheet 164, North Central Nigeria

Abbas Muhammed^{1*}, Onoduku Usman Shehu¹ and Ako Thomas Agbor¹

¹*Department of Geology, Federal University of Technology, Minna, Nigeria.*

Authors' contributions

This work was carried out in collaboration between all authors. Authors AM and OUS designed the study, performed the statistical analysis, wrote the protocol, and wrote the first draft of the manuscript. 'Author AM' managed the analyses of the study. Authors AM and ATA managed the literature searches. All authors read and approved the final manuscript.

Article Information

DOI: 10.9734/AJOGER/2018/41835

Editor(s):

(1) Dr. Ntokozo Malaza, Department of Occupational and Environmental Studies, Faculty of Applied Sciences, Cape Peninsula University of Technology, Cape Town, South Africa.

Reviewers:

(1) Nforba, Melvin Tamnta, School of Geology and Mining Engineering, University of Ngoaundere, Cameroon.

(2) Pavel Kepezhinskas, USA.

Complete Peer review History: <http://www.sciencedomain.org/review-history/26675>

Original Research Article

**Received 09 April 2018
Accepted 19 June 2018
Published 15 October 2018**

ABSTRACT

The study investigates the geological and geochemical characterization of rocks in an area of about 21 km² in vicinity of Kuta North Central Nigeria with a view to identify the relationship between the rock units, the petrographic characteristics of the rock assemblages, their original protoliths, and geochemical characterization of the rocks. Field and laboratory works such as: petrography, X-ray Fluorescence (XRF), and X-ray Diffractometer (XRD) have revealed that the study area is entirely underlain by metasedimentary Precambrian pelitic rocks characterized mostly by mica schist, quartzite ridge complex (in NE-SW direction), quartz-kyanite schist, and Banded Iron Formation (BIF). The discrimination diagrams constructed reveal the following: greywacke, tholeiitic, and arc related origin of the mica schist; tholeiitic with meta-arkosic nature of the quartzite; the hybrid sedimentary-igneous protolith (greywacke and arkosic) nature of the quartz-kyanite schist; and the terrigenous and submarine hydrothermal for the BIF. The petrographic and XRD study indicate that the mica schist consist of quartz, phlogopite, paragonite, muscovite, kyanite, topaz, rutile, kaolinite, and magnetite assemblages and quartzite consist mostly quartz, topaz, kyanite, and rutile. The quartz-kyanite schist consist quartz, kyanite, muscovite, topaz,

*Corresponding author: Email: abbasmuhammed16@yahoo.com;

paragonite, kaolinite, rutile, and hematite, while and the BIF composed of magnetite, quartz, hematite, and rutile.

The mean percentage of the major defining chemical elements (such as alumina and silica) for kyanite mineralization potential rocks according to standard requirements of kyanite for industrial use, indicates that the rocks contain a very low amount of alumina with higher percentage values of deleterious elements such as SiO_2 , Fe_2O_3 , TiO_2 , $\text{Na}_2\text{O}+\text{K}_2\text{O}$ and $\text{MgO}+\text{CaO}$. The mineralogical analysis (via XRD) and modal analysis during petrographic studies show that the percentage composition of kyanite in the kyanite bearing rocks is greatly below the acceptable limit when compare to other economic kyanite deposits around the world.

Keywords: *Metasedimentary; kyanite-bearing rocks; Kuta; Precambrian pelitic rocks; ridges; deleterious; standard; economic.*

1. INTRODUCTION

The study area is part of North-Central segment of the Nigerian Basement complex and forms part of the Kuseriki Psammite Formation. The Kuseriki Psammite Formation includes migmatites and other three notable members, each of distinctive lithology [1]. These are the quartzites of the Kubo member, the kyanite-schist and quartzites of Tungan Bargwoma member, and the granulitic rocks of Zungeru member; ages in the Kuseriki Schist Group have been estimated to be Kibaran ($1,159 \pm 70$ Ma) by Truswell and Cope [1]. The Schist belts compose the most remarkable structural pattern in the Precambrian Basement Complex of Nigeria.

The Nigerian basement occupies the reactivated region which resulted from plate collision between the passive continental margin of the West African craton and the active Pharusian continental margin [2]. The basement rocks are considered to be the products of at least four major orogenic cycles of deformation, metamorphism and remobilization corresponding to the Liberian (2,700 Ma), the Eburnean (2,000 Ma), the Kibaran (1,100 Ma), and the Pan-African cycles (600 Ma) [2]. Within the basement complex of Nigeria four major petro-lithological units are differentiated, namely: The Migmatite – Gneiss Complex (MGC), the Schist Belt (Metasedimentary and Metavolcanic rocks), the Older Granites (Pan African granitoids), and undeformed Acid and Basic Dykes [2].

The schist belts were formerly referred to as the “younger meta-sediments” to differentiate them from the migmatitic gneisses which were termed the “older meta-sediments” [3]. They constitute distinct NE-SW trending belts of schists generally believed to be Upper Proterozoic which are clearly younger and infolded into the migmatite-

gneiss-quartzite complex [1]. These meta-sediments consist of low to medium grade mica schists, quartz schist, quartzites and concordant amphibolites. In the southwestern Basement Complex, the belt is associated with marbles, dolomites and calc-silicate rocks [4]. The northwestern Basement Complex is mostly dominated by schists of greywacke origin made up of meta-pelites and quartzites, phyllites, mica-schists, quartzo-feldspathic schists, paragneiss, Fe-Mn rich quartzites and garnet amphibolites [4]. The metamorphosed pelitic to semi-pelitic rocks of Anka, Birnin Gwari and Zungeru schist belts contain interbedded acid and intermediate extrusive rocks. Similar to other schist belts notably in the northwest Nigeria, the rock units form unique discrete belts with distinct and contrasted lithologies, separated by either the migmatite-gneiss complex or the Pan-African granitoids [2].

The study area lies between latitude $9^\circ 51'$ to $9^\circ 05'3''\text{N}$ and longitudes $6^\circ 42'$ to $6^\circ 04'5''\text{E}$ which covers an area of approximately 21 km^2 mapped on a scale of 1:12,500 (Fig. 1).

Kyanite occurs as elongated prismatic crystals in gneiss, schist, pegmatite, and quartz veins as a result of high pressure regional metamorphism of principally aluminous rocks [5]. It occurs in the form of kyanite quartzite, kyanite schist, kyanite gneiss, quartz-kyanite pod, and as detrital grain in sedimentary rocks. Truswell and Cope [1] noted the occurrence and widespread of kyanite schists and gneisses in highly metamorphosed regions of the Nigeria basement complex. The basement complex of the study area is characterized by mica schist; intruded by quartzite forming a ridge in NE-SW direction; quartz-kyanite schist; and the occurrence of Banded Iron Formation (BIF) overlying the Precambrian pelitic rocks, all of sedimentary origin. The interleaved and gradational contact relationship of the mica schist with quartzite and

between the quartz-kyanite schist indicates sediment deposition under unstable flow regimes [6].

Kyanite is a member of the aluminosilicate series strongly anisotropic that its hardness varies depending on its crystallographic direction which can be considered as distinctive characteristics used to differentiate it from other aluminosilicate polymorphs [7]. Geochemical evidence can be used to show the most widespread kyanite rich rock due to mobility of some chemical elements which may be concentrated in kyanite bearing rock and show depletion in the other rocks that are not kyanite rich [7]. Kyanite is a common mineral in three lithological units around Kuta north central Nigeria, and exists as the only Al_2SiO_5 polymorphic mineral disseminated in veins, quartzite, and rocks of higher metamorphic grade (such as mica schist and quartz-kyanite schist); and topaz occurs as the only anhydrous aluminium-silicate mineral associated with the kyanite bearing rocks .

The world resources of kyanite minerals are large, but few of these are in the form of high grade, coarse grained material which is valued as industrial raw materials; and the most common and usable types are the lump massive and lenses in metamorphosed aluminous sediment, as stratiform replacements within foliated and non-foliated quartzose rocks, mineralized quartz veins and pegmatites, and in residual soils and placers [8]. Due to the qualities of hardness, durability, and resistance to heat and chemical corrosion makes kyanite a valuable mineral used mostly in the manufacture of high alumina, high performance refractories, especially in monolithic refractory applications [8]. It is used in iron and steel industries; glass and nonferrous metals to increase the production, in cement and binders to counteract shrinkage, as fertilizers for agricultural use, and in kiln furniture to offset shrinkage from clay in order to provide economic source of mullite at higher temperature that is beneficial [8]. Kyanite minerals can also be used as mold coatings in foundry industry where gas permeability is an important criterion, as electrical insulators, abrasives, and as semiprecious gemstone which may display cat's eye chatoyancy

The geochemistry and mineralogical evaluation of quartzite bearing kyanite in Kuta, Northwestern Nigeria has been studied by Omang and Alabi [9]. They reported that they are low to medium grade metamorphic rocks that range from the kaolinite to the biotite isograde,

delineated by their mineral assemblages. The rocks generally trends NE-SW direction and consist of quartz, kyanite, phlogopite, and paragonite as the chief minerals. The other associated minerals include magnetite, rutile, topaz, muscovite, kaolinite, and hematite. The present study is hoped to assist in understanding the geological and geochemical characterization of kyanite-bearing rocks around Kuta, in order to serve as a guide for future exploration purposes in the study area.

2. MATERIALS AND METHODS

The methods for this study consisted of field work and laboratory study. During the field exposures of the different rock types which occur along river valleys, road-cuts, as well as on hill sides. In the field, each outcrop was observed and described based on its mode of occurrence, macroscopic characteristics, structural elements and field relation with adjacent outcrops. Hand specimens were described (based on the colour, texture, mineralogy) and were carefully labelled, points plotted on the base map at the appropriate locations where the samples were collected with the use of a Garmin Global Positioning System (GPS) and the geographic coordinates of the base map was done. Careful observation of lithological boundaries or contacts was made by observing changes in rock exposures, nature of soil, vegetation and topography. A Silva compass clinometer was used to measure joints on the outcrops which were plotted on the rose diagram to give a principal joint direction of NE-SW, fault angles, strike and dip values, and directions of outcrops using the contact method were delineated. During the field work, ten representative samples were selected and collected from the different rock units encountered in the study area. Two samples were selected from quartz-kyanite schist, quartzite, and BIF and four from the mica schist. The samples collected from the field were used for thin section preparation and petrographic study, Mineralogy and chemical analysis.

The thin sections were prepared at the Geology Department laboratory, Kogi State University, Ayingba, Nigeria. In preparing the thin section a thin slide of rock was cut from each representative samples using a diamond saw and ground optically flat with 400 grit carborundum. The glass slides used for each sample were grinded to make their surface rough to fix the rock samples onto the slides. The samples were then mounted on the rough glass slide using epoxy resins to glue the samples to

the glass slides, and then lapped, ground smooth using progressively finer abrasive (600 grit carborundum), and polished to the required thickness and surface finish, approximately 30 micron. The slides were removed and cleaned and they were now ready for study. The slides obtained were studied under Transmitted Polarized Light Microscope. Typically quartz was used as the gauge to determine thickness as it is one of the most abundant minerals in the samples. The thin sections produced were studied using polarizing petrographic microscope of the Department of Geology, Federal University of Technology, Minna, Nigeria. Fifteen (15) representative rock samples were also selected and prepared for mineralogical and elemental analyses, with the aid of X-ray diffraction (XRD) and X-ray fluorescence (XRF) machines respectively.

Fifteen (15) representative rock samples were also selected and used for mineralogical and elemental analyses using X-ray diffraction (XRD) and X-ray fluorescence (XRF) methods respectively. The results of the chemical or elemental analyses were further plotted on various geochemical discrimination diagrams and compare with those of similar studies to elucidate the kyanite bearing rocks in the study area. For whole-rock geochemistry, the major oxides and the trace elemental concentrations in the samples were determined using X-ray fluorescence (XRF) method at Engineering Materials and Development Institute (EMDI) Akure, Ondo State. In this method glass beads were prepared for major elements determination in the geological samples (such as: Si, Al, Fe, Ca, Mg, Na, and K in addition to Ti, Mn and P). A 0.4 g of part of each sample was mixed with 7.5 g part of Spectroflux 100 (Li-tetraborate) to give all samples a similar matrix and to make the melting process easier. The mixture of each sample with flux were melted separately using air acetylene flame at 1150⁰ C for about 15 minutes in a crucible made of Platinum (Pt) with 5% gold (Au) to let the melt drop from the crucible more easily. A special machine for melting was programmed to the right melting temperature, time, and agitation. The melting process in the machine ends by casting the melt of each particular sample in a Pt/Au form or plate and air cooled. The homogenous beads then were released from the forms and numbered for easy identification during XRF analysis. Sample materials were ignited, and loss on ignition (LOI) is determined before mixing with flux. Loss on ignition is used for correction of

results of the analysis to represent the original (not ignited) materials. The LOI was done gravimetrically by weighing 1 g of the pulverised rock sample into platinum crucible of known weight using a weighing balance. It was then subjected to temperature of about 1000⁰C using air acetylene flame. The content was allowed to cool and then weighted to represent the original (not ignited) material. Pressed powder pellets were prepared for determination of low concentration elements of high atomic number, called trace elements (10 to 100s ppm). 10 g of each rock sample (finely grounded to <50 µm to prevent analytical problems due to grain size effects) was weighed in an agate mortar and 2 ml Elvacite solution (purely organic compound of Methyl-butyl methacrylate) was added as cellulose binder. It was mix well with a pestle until the powder is completely dry, and there exist a very thin film of Elvacite around each grain. The sample was placed in the form and pressed with a load of 20 tonnes. The sample was released from the form and was placed in an oven at 80⁰ C for about 1 hour to harden it. The form was cleaned and washed with ethanol after use to prevent oxidation, and a different part of it was wrapped in paper for storage. The process above was repeated for the other fourteen samples for use this method.

The samples for XRD analysis to determine the mineral constituents of the rocks were prepared and analysed at the National Geosciences Research Laboratories (NGRL) of Nigeria Geological Survey Agency, Kaduna, Nigeria. In order to obtain an ideal diffraction pattern of a mineral each sample was grinded and sieved to <270 mesh in order to obtained a crystalline smooth surface powder pressed into the sample holder at an angle of 45⁰. Little Smasher was used to reduce the size of larger chips of sample to approximately sand-size (less than 1 or 2 mm), and about 2 g of the coarse grind was transferred into the steel container of about 20% full for grinding in the spex mixer. A steel ball or form was added to the container and the lid was put on. The grinding container was mounted into the mixer, fasten snugly, close the lid and the mixer was turn on for at least 5 minutes depending on the hardness of individual specimen. After the grinding was completed, the powders were transferred to a piece of weighing paper and sieved through the 270 mesh sieve, and the grinding vessels were cleaned with a Kim wipe and acetone. The powder in the sample holder was mounted with a clean

material according to the procedure in the Philips manual.

3. RESULTS AND DISCUSSION

3.1 Lithology and Petrography

The studied area has an antiformal structure with four lithologic units comprising mica-schist, quartzite ridge, quartz-kyanite schist, and subordinate Banded Iron Formation (BIF) as shown in Fig. 1. The basement rocks comprise a series of metamorphosed complex of mica-schist intruded by a narrow ridge quartzite outcropping over 360 m high, quartz-kyanite schist, and BIF deposit, all of sedimentary origin.

Joint values of rocks from the area are presented in Table 1 and plotted on rosette diagram (Fig. 2) to decipher the structural trending exhibited by the rocks. A dominant NE-SW structural trending is shown on the rosette diagram (Fig. 2). The minor structural fractures of the rocks exhibit NW-SE trending as indicated in Fig. 2.

The contact relations among the rock types are obliterated by metamorphism and deformational episode, hence, integration of obvious lithological difference, metamorphic extents, field appearances and structural styles were used to classify the rock succession of the area into units as described below.

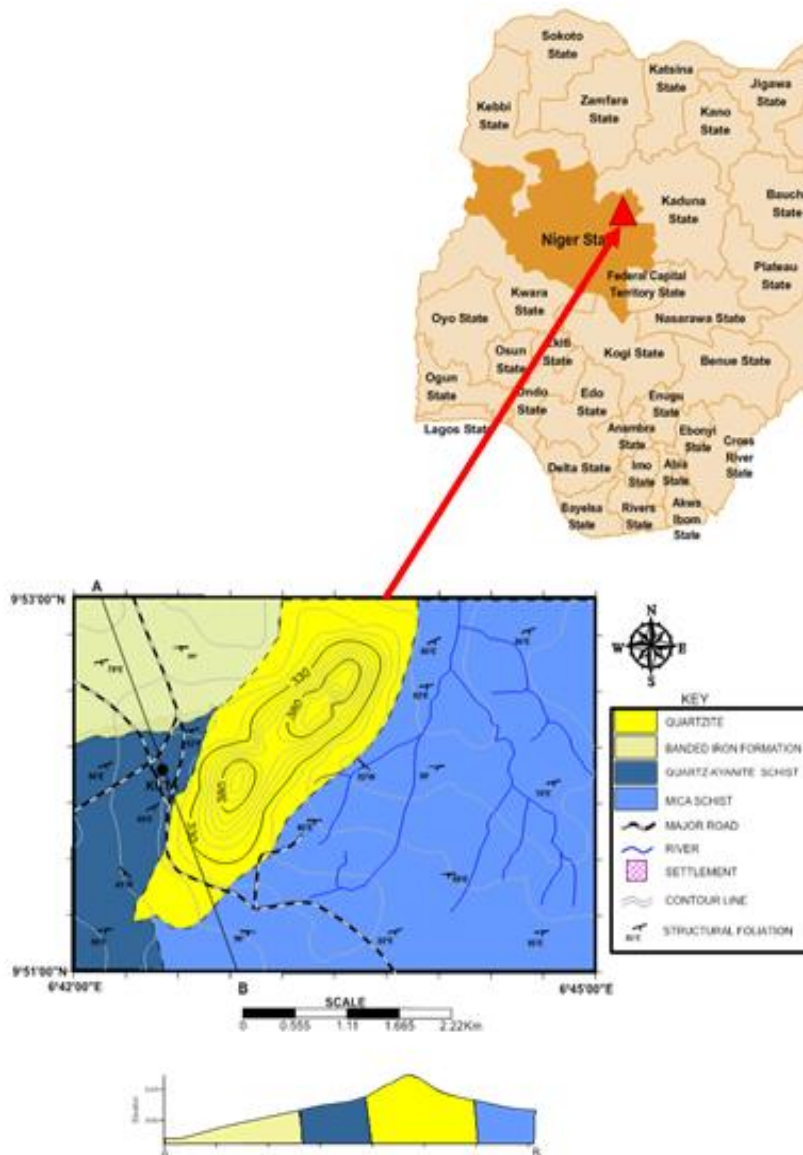


Fig. 1. Geological map of the study area

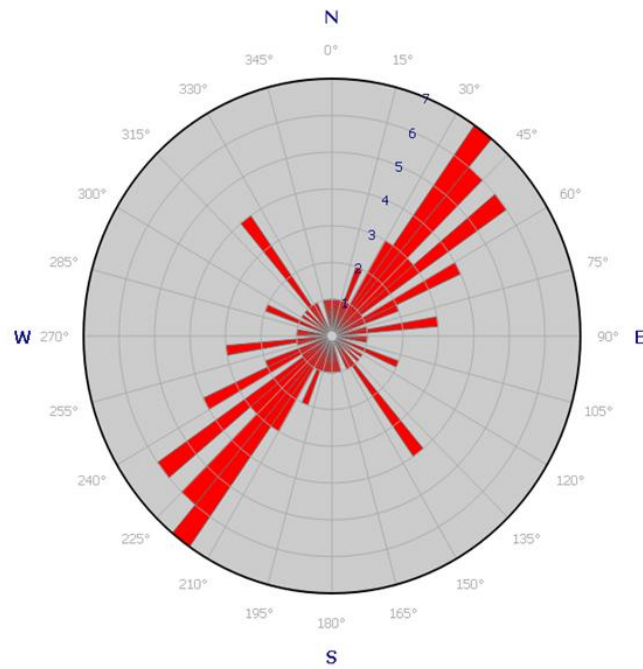


Fig. 2. Rosette diagram of joint pattern of rocks around the study area

Table 1. Joint direction and frequencies of rocks around the study area

Joint direction	Frequency (F1)	Joint direction	Frequency (F2)	Total (F1+ F2)	Percentage $(F1+F2) \times 100$ total
000° - 030°	5	181° - 210°	4	9	15.5
031° - 060°	17	211° - 240°	10	27	46.6
061° - 090°	7	241° - 270°	1	8	13.8
091° - 120°	1	271° - 300°	3	4	6.9
121° - 150°	1	301° - 330°	6	7	12.1
151° - 180°	1	331° - 360°	2	3	5.2
Total	32		26	58	100

3.1.1 Mica schist

The mica schist is a grey to light reddish coloured rock of fine to medium grain texture widely distributed banded rock unit. The rocks often disclose a typical low to medium grade mineral assemblage comprising phlogopite-muscovite-paragonite-quartz-rutile-topaz. The rocks are highly deformed and display conspicuous segregation into light and dark portion with well-defined schistosity. Intensive plastic deformation of metric in size folds are observed in the rock formation. This plastic rock matrix of monomineral lenses up to 3 cm in width is build-up of quartz which is parallel to the main metamorphic foliation. The aluminosilicate portion contains porphyroplasts of kaolinite, muscovite, paragonite, kyanite, and topaz which is generally thicker than the dark portion. The

dark portion consists of mafic phyllosilicate minerals dominanatly phlogopite.

The mica schist is also fractured and the fractures which dominantly trends 110° with nearly vertical dips of 70°- 90° to the northeast, cut the schistosity, Fig. 3 (a). The foliation of this rock trends NE-SW, most of the fractures are closed; infilling some fractures are schistose material, quartz and feldspar to form quartzofeldspathic veins as seen in Fig. 3 (b), and deposition of such in-filling materials is facilitated by volatile transport.

In thin section, the mica schist is seen as a fine to medium grained with some degree of schistosity and mineral lineation. The plane polarized light (PPL) shows the phlogopite to occur as dark brown flakes with one plane of the

phlogopite associated with muscovite and paragonite minerals. The present of rutile and topaz are due to silica loss. The kyanite minerals present, are prismatic to tabular in shape which displays simple twin and cleavage occurrences as seen in Fig. 4(d) under cross polarized light (XPL). The rutile is strongly pleochroic in shades of red-brown and the crystal form is subhedral to anhedral with interference colour often veiled by strong absorption.

The quartz mineral grains vary in sizes from large to small (0.5 to 1.0 mm) in length with some having preferred orientation. There is widespread undulose extinction in the quartz grain as seen under XPL. Inclusion of water and melt forming haloes; and vein deposit having a core enriched in disseminated kyanite and progressively deplete in kyanite to the rim as seen in Fig. 4 (a & b).

3.1.2 Quartzite

The quartzite occur in the central part of the area as relatively outstanding ridges trending in a NE-SW direction for considerable distance probably tracing a linear regional pattern representing fault zone.

The quartzite is a well-defined continuous outcrop of most likely to be high grade

metasedimentary. The sedimentary origin of this suite is notable in the field by it heterogeneous nature, prevalent intercalation feature, with over 360 m high developed in area of about 4 km²; and short distance facies change established by the geochemical and petrographic data. There is sufficient field evidences for inferred contact relations between the quartzite, quartz-kyanite schist, the Banded Iron Formation, and the mica schist. The quartzite is compact, brecciated rock varying from smoky white to ferruginous reddish brown or grey colour diversity, Fig. 5 (b). In hand specimen the quartzite shows abundant quartz crystals, few muscovite flakes, k-feldspar, ferromagnesian minerals, and opaque.

In thin section (Fig. 6), the quartzite is seen as a very fine grained subhedral to euhedral equidimensional quartz crystal with minor amount of opaque minerals and significant amount of resistance minerals such as topaz and rutile which may also indicate silica loss. Rutile formed an inclusion within the quartz crystal which form a dense tabular to prismatic fibre. This type of combination is known as rutilated quartz which may indicates some degree of titanium mobility. As seen in Fig. 6 (d), kyanite which form a simple twin crystal within the quartz crystal account for about 20% in the thin section.

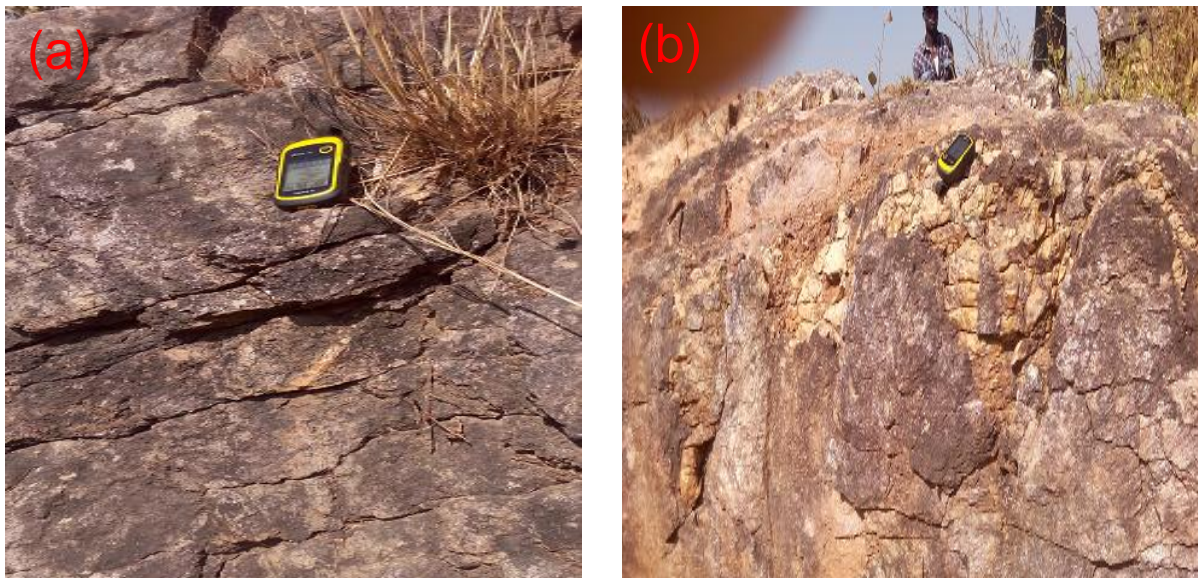


Fig. 3. (a) Mica schist showing joint system; and (b) Mica schist with massive veining

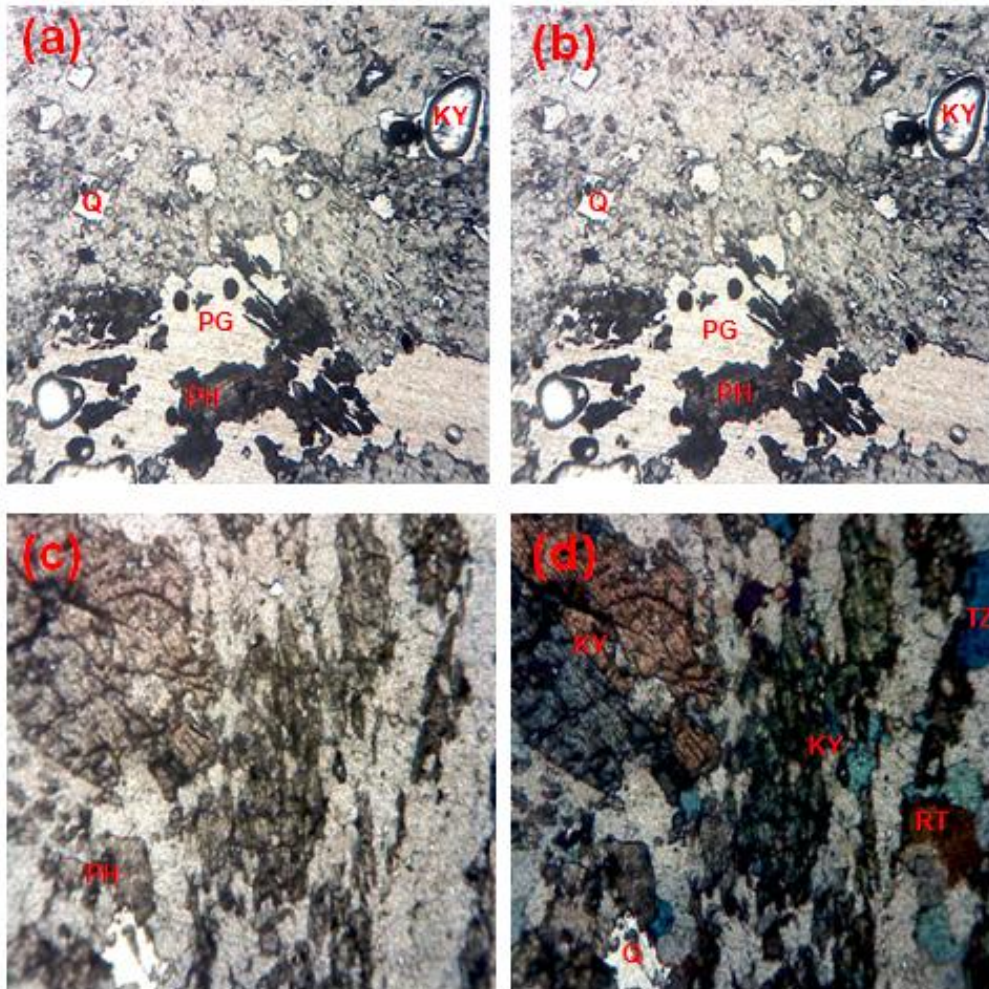


Fig. 4. Photomicrograph of mica schist under (a & c) plane polarized light and (b & d) crossed polarized light showing Quartz (Q), Phlogopite (PH), Paragonite (PG), Kyanite (KY), Topaz (TZ), and Rutile (RT), Magnification= X10

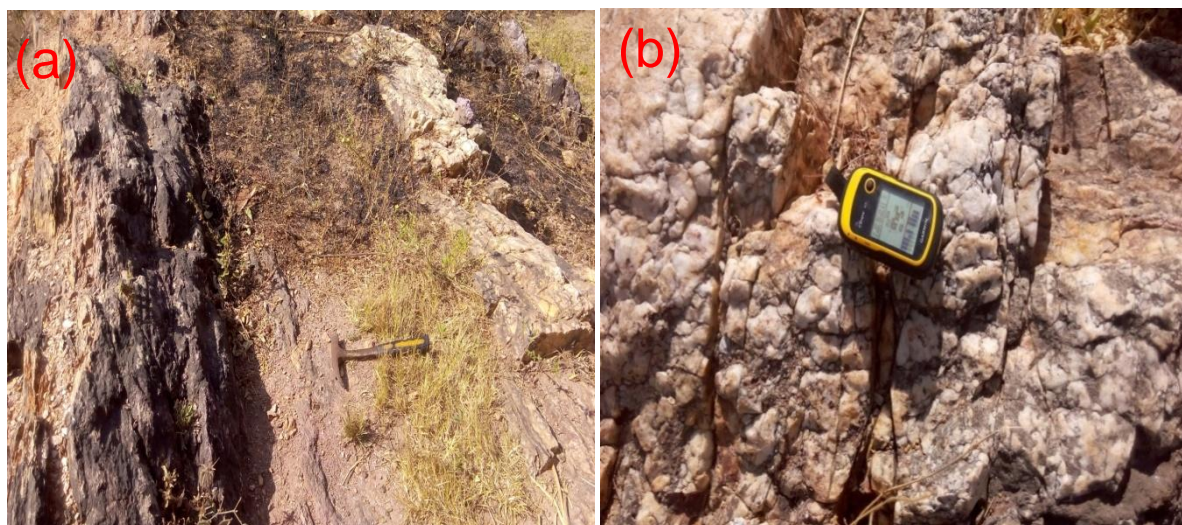


Fig. 5. (a) Intercalation of mica schist and quartzite contact exposure; and (b) Smoky white to ferruginous reddish brown fractured quartzite

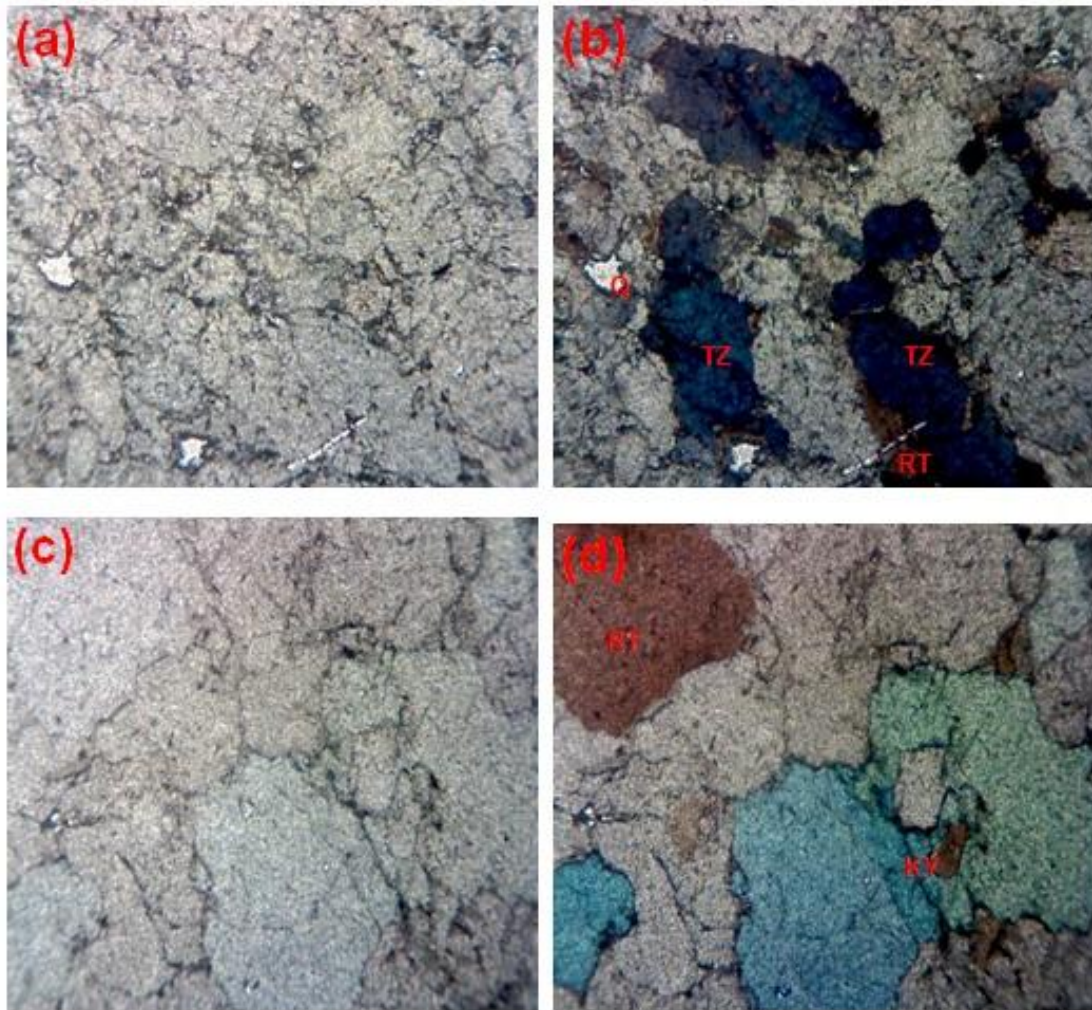


Fig. 6. Photomicrograph of quartzite under (a & c) plane polarized light and (b& d) crossed polarized light showing Quartz (Q), Kyanite (KY), Topaz (TZ), and Rutile (RT), Magnification= X10

3.1.3 Quartz-kyanite schist

A sequence of quartz-kyanite schist structurally overlying the mica schist in the area locally contains thin psammitic banks which may represent original sedimentary layering. It is a light coloured rock with flaky alignment of muscovite, kyanite and other minor phyllosilicate minerals such as paragonite and kaolinite with less developed schistosity. The thickness of strips enriched in these minerals few millimetres up to 1-2 cm.

The rock is dominantly rich in aluminosilicate minerals with evidence of quartz veining and very low traces of iron oxidation, the quartz-kyanite schist generally trends NE-SW direction in the north westernmost part

of the area where its presence is most prominent.

Intensive plastic deformation is observed in the rock formation of metric in size folds, characteristics of highly plastic rock matrix monomineralic lenses up to 2 cm in width, composed of quartz parallel to the main metamorphic foliation, as seen in Fig. 7 (b). Irregular distribution of the main rock forming minerals quartz, kyanite, muscovite and kaolinite is the characteristic feature of the rock. In thin section, quartz-kyanite schist occurs as a fine grained with some degree of schistosity. Quartz constitutes over 70% of the mineralogical assemblage with minor kyanite, kaolinite, muscovite, pinitized phlogopite, and paragonite as well as occasional rutile and opaque minerals (Fig. 8).

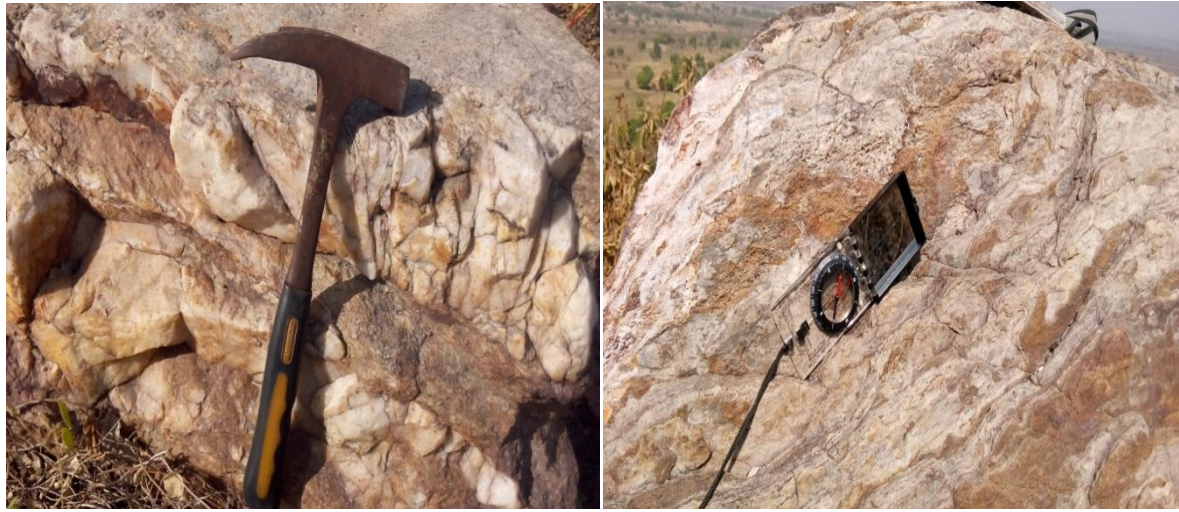


Fig. 7. (a) Intrusion of quartz within the quartz-kyanite schist; and (b) quartz-kyanite schist outcrop with plastic deformation displaying microfold

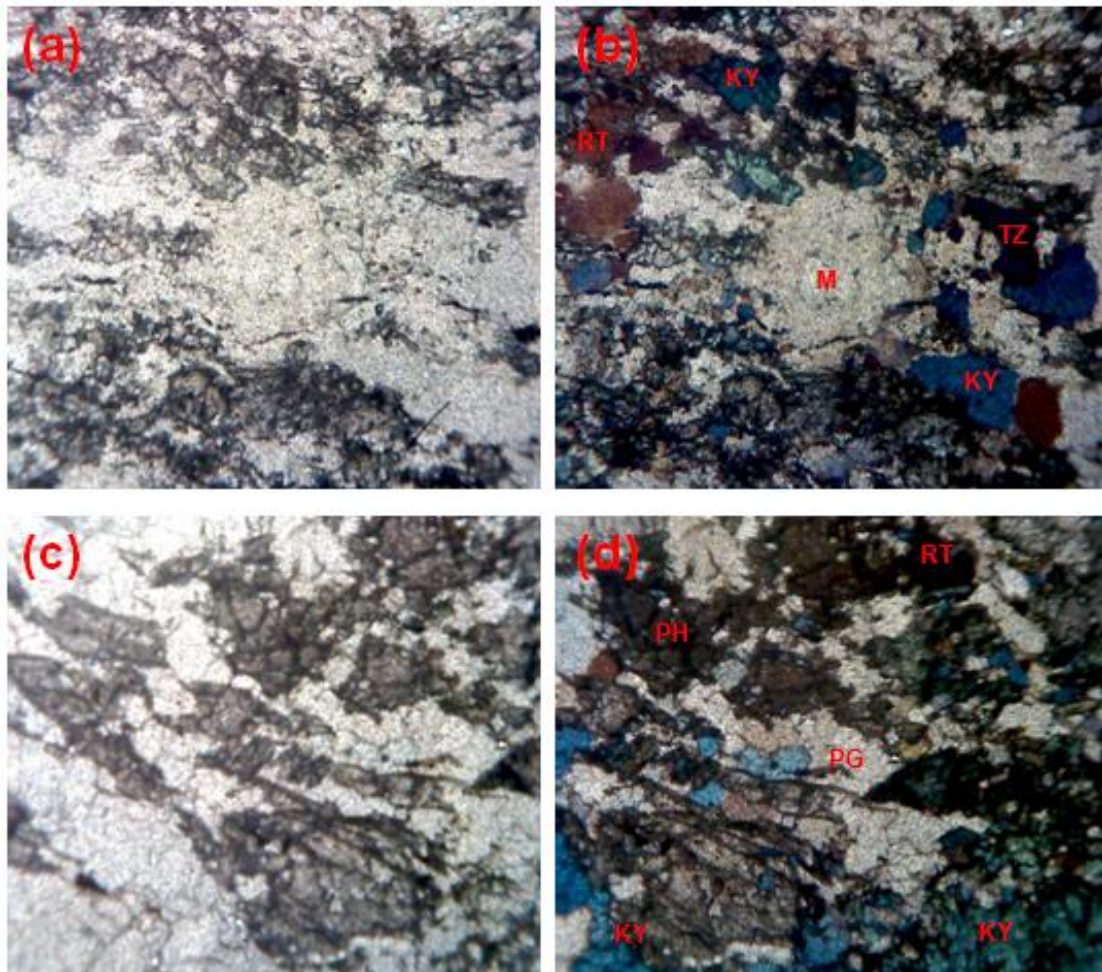


Fig. 8. Photomicrograph of Quartz-kyanite schist under (a & c) plane polarized light and (b & d) crossed polarized light showing Quartz (Q), Muscovite (M), Paragonite (PG), Phlogopite (PG), Kyanite (KY), Topaz (TZ), and Rutile (RT), Magnification= X10

3.1.4 Banded Iron Formation (BIF)

The uppermost north-western part of the area which trends N-S is dominated by extensive ferruginized metasediments known to be Banded Iron Formation (BIF).

The tabular BIF extending for distances from hundreds of meter to over 1 km frequently displayed minor faulting, is a finely bedded sedimentary rock with anomalously high iron content interbedded with the pelitic schists.

The BIF is dark reddish brown to grey banded rock with alternation of light grey rich silica and darker iron-oxide rich bands. It is of heterogeneous variety and occurs as boulders of different sizes ranging from 15 cm to 4 m intercalated within the surrounding rocks (Fig. 9). Magnetite and hematite are the major ore constituents in variable percentages.

Quartz, magnetite, and hematite were identified in the thin section. The light coloured mineral is quartz, while the dark coloured grains are magnetite and haematite. Quartz crystal occurs as interlocking mosaic and as inclusions within haematite and magnetite (Fig.10). Fractures in the quartz crystals indicate the effect of post-deformational disturbances.

3.2 Geochemical Results

Each sample was analysed for major elements and trace elements, and the whole-rock geochemical data of the representative samples of rocks were used to categorize them in terms of origin. The geochemical results of rocks encountered on field in the area are presented in Tables 3 and 4.

Chemical analyses are essential mainly for comparing rocks and mineral deposits in order to elucidate possible degree of variation within them in the study area. These data are used in construction of different types of variation and discrimination diagrams; in combination with the field and petrographic evidences, the rocks in the study area were classified.

The chemical results of the rock samples show that some major element concentrations cover a broad compositional range which suggests diverse protolith [6]. As shown in Table 3. SiO₂ content is highest in the quartzite, followed by quartz-kyanite schist, mica schist, and BIF contains the least concentration with values ranging from 90.01-94.60 wt % averaging 93.14 wt %, 91.70-66.60 wt % averaging 80.22 wt %, 47-60 wt % averaging 54.08 wt %, and 27.52-28.34 wt % averaging 27.93 wt % respectively for



Fig. 9. (a) Extensive heterogeneous varieties of BIF boulders; and (b) Intercalation of heterogeneous BIF boulders with highly weathered mica schist

the four rock types. This is followed by high to moderate Al_2O_3 content ranged between 19.60-34.90 wt%, 19.05-6.13 wt%, 0.74-10.08 wt% with an average of 27.08 wt %, 12.59 wt %, and 7.23 wt % for mica schist, BIF, and quartz-kyanite schist respectively, while the concentration of the Al_2O_3 in quartzite samples is low at 1.99 wt % average. Though, it is similar to the average concentration of Al_2O_3 obtained from Okemesi quartzite [10]; and that of Itawure quartzite [11].

The K_2O/Al_2O_3 ratios for the mica schist in this study are within the range of 0.0 and 0.3; this suggests the enrichment of significant amount of clay minerals [12]; and this claim is also supported by Adedoyin et al. [6] who envisaged that the high aluminium enrichment reflects the control of their composition by aluminous clay minerals.

Generally, the concentrations of P_2O_5 , Na_2O , K_2O , CaO , MgO , MnO , TiO_2 , and Fe_2O_3 for the rock samples are low, except the Fe_2O_3 content of the BIF which shows anomalous concentration of 47.08-59.10 wt% with an average value of 53.09 wt%. The high Fe_2O_3 value may be ascribed to supergene enrichment due to impregnations and replacements related to post-metamorphic processes as envisaged by Adekoya [13], who suggested it was as a result of leaching and redeposition of oxide within the enrichment zone. The increase of Fe_2O_3 with a decrease in Al_2O_3 may indicate replacement of precursor silica with goethite, which later dehydrated to hematite [14]. This is also similar to the observation of Mucke and Nuemann [15] on the BIF of Itakpe area.

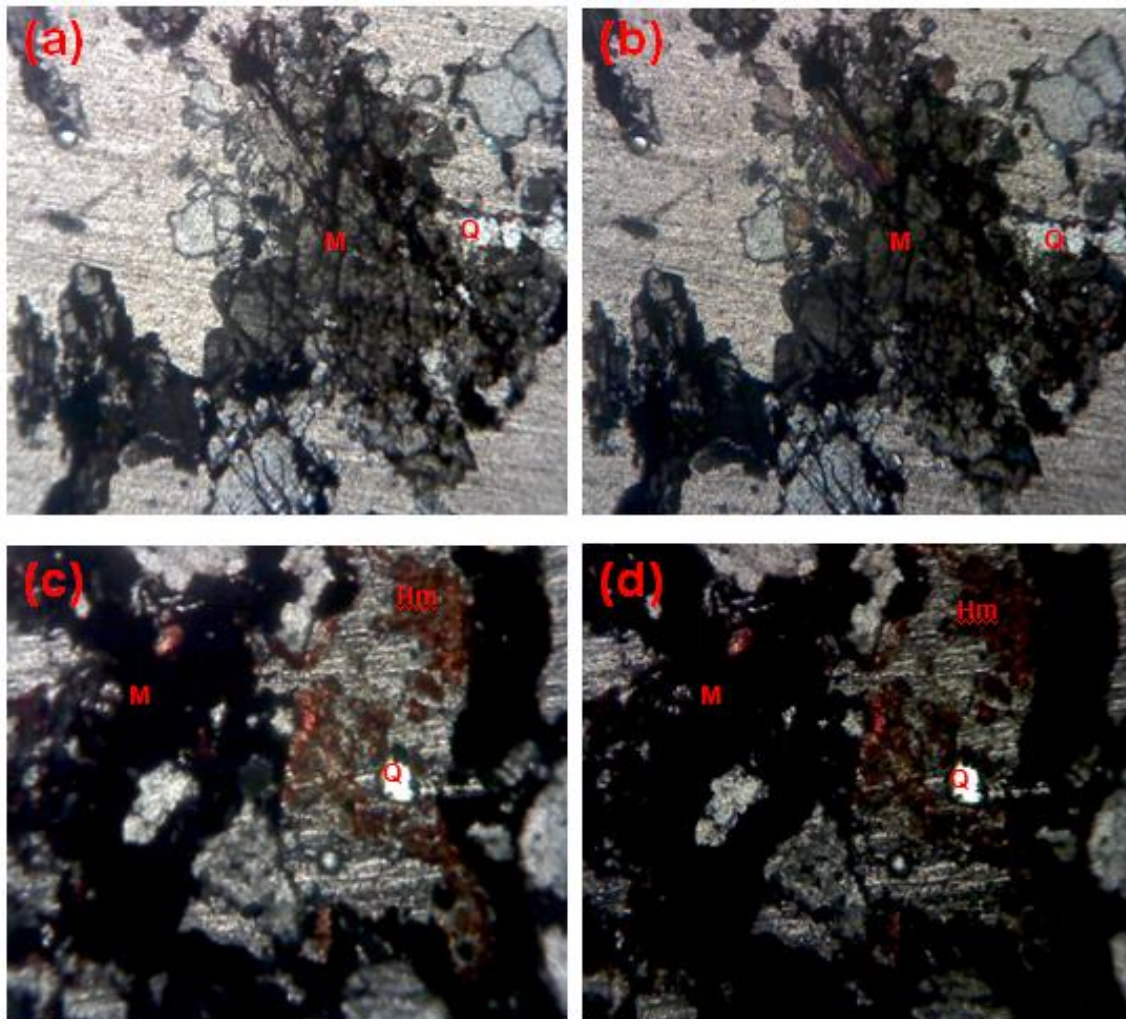


Fig. 10. Photomicrograph of Banded Iron Formation (BIF) under (a & c) plane polarized light and (b & d) crossed polarized light showing Quartz (Q), Magnetite (M), Hematite (Hm) Magnification= X10

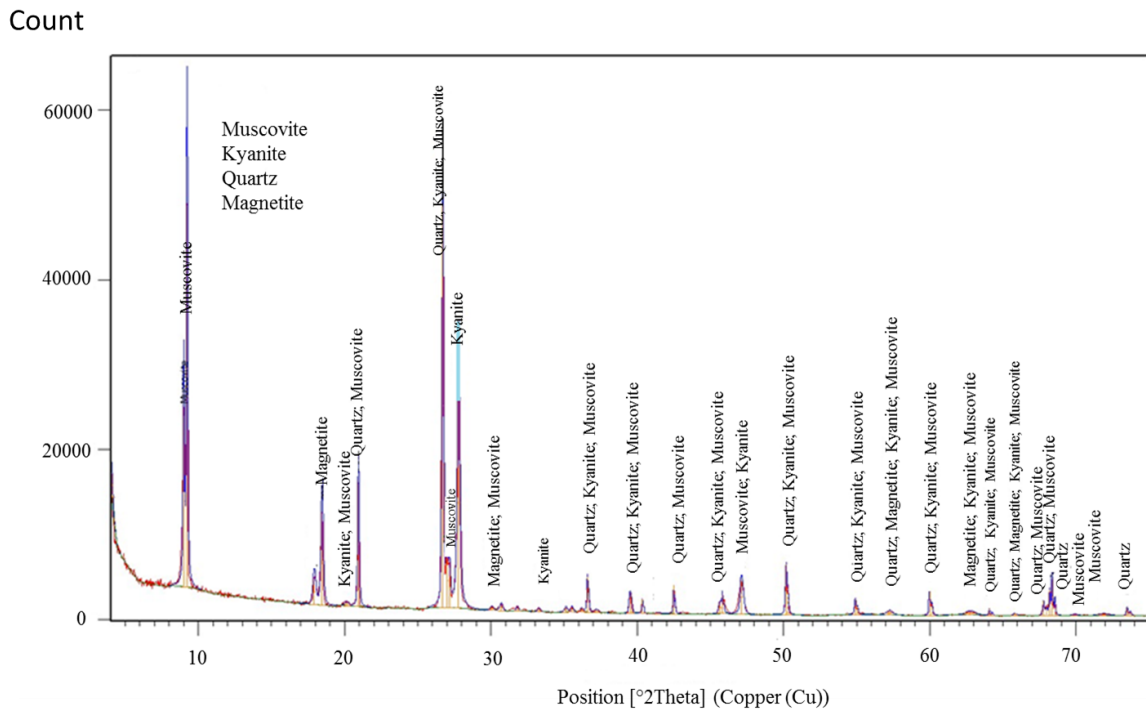


Fig. 11. Diffractogram of sample AM13 (Quartz-kyanite schist)

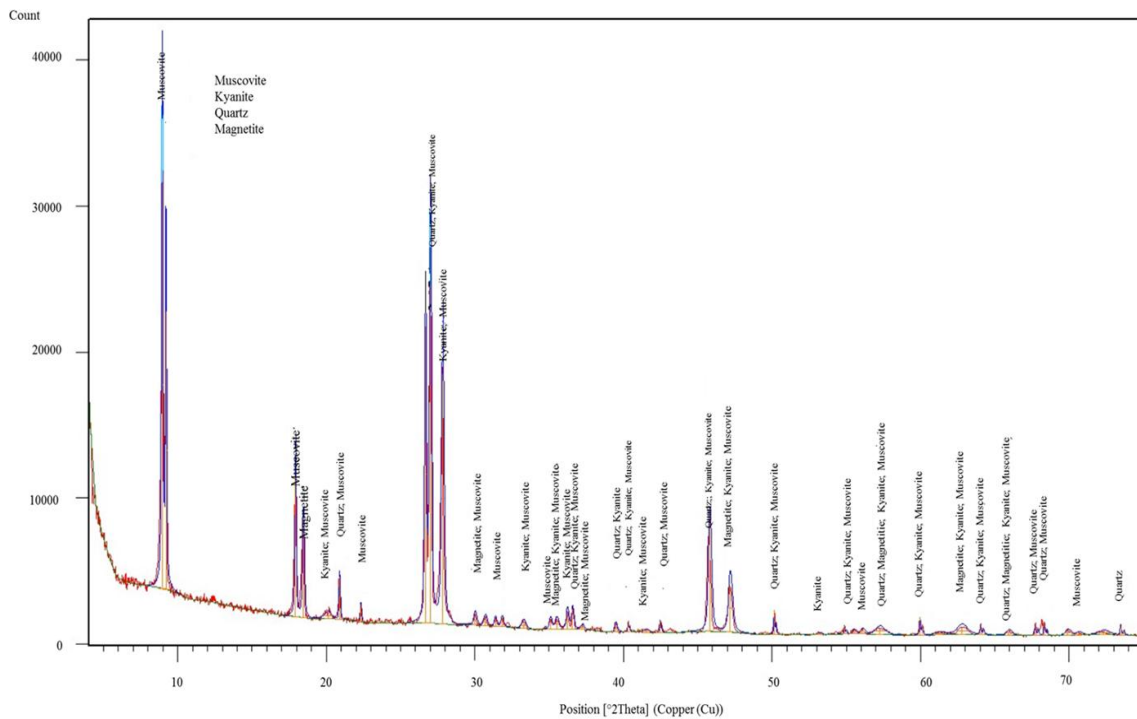


Fig. 12. Diffractogram of sample AM03 (Mica schist)

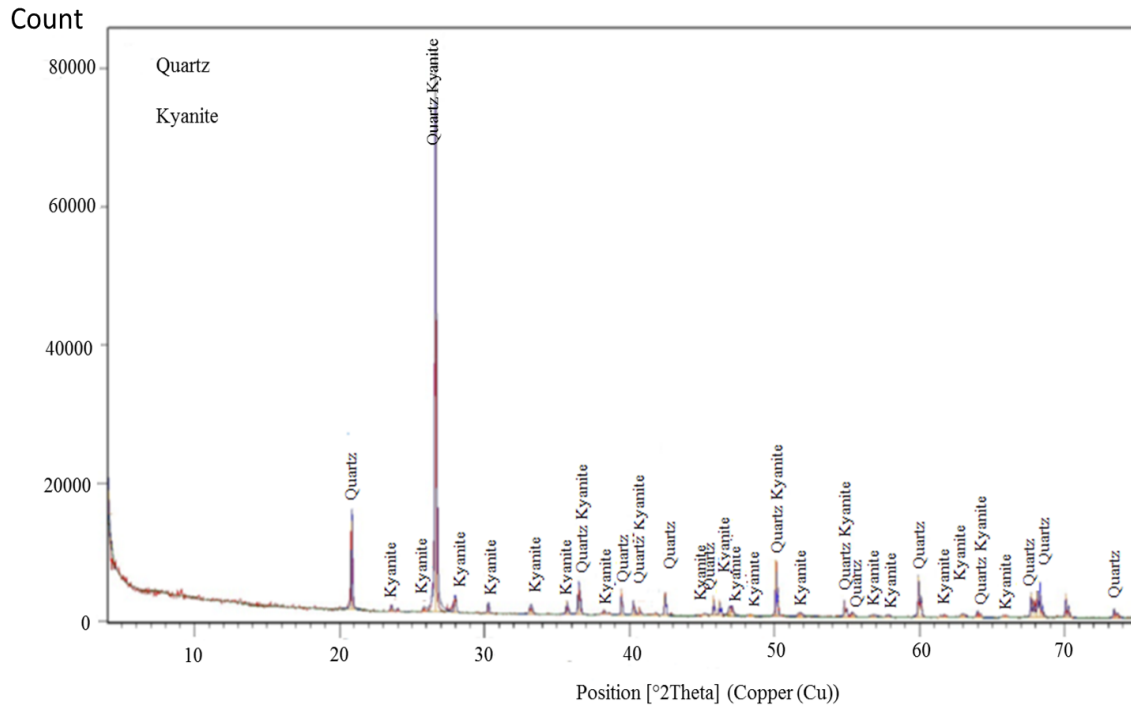


Fig. 13. Diffractogram of sample AM11 (Quartzite)

Table 2. Mineral compositions of rocks around the study area on the basis of XRD analysis

Samples	Lithology	Major constituent	Minor constituent
AM01	Quartzite	Quartz + kyanite + topaz	Rutile
AM02	Quartzite	Quartz + topaz + rutile	Kyanite
AM03	Mica schist	Quartz + muscovite + kyanite + magnetite	
AM04	Mica schist	Quartz + kyanite + topaz + rutile	Magnetite
AM05	Mica schist	Quartz + kyanite	Topaz + rutile
AM06	Mica schist	Phlogopite + paragonite + quartz	Kyanite
AM07	Quartz-kyanite schist	Quartz + kyanite + topaz	
AM08	Quartz-kyanite schist	Quartz + kyanite + paragonite + kaolinite	Rutile
AM09	BIF	Magnetite + quartz + hematite	
AM10	BIF	Magnetite + quartz + hematite	Rutile
AM11	Quartzite	Quartz + kyanite	
AM12	Mica schist	Quartz + rutile + topaz	Paragonite + kyanite
AM13	Quartz-kyanite schist	Quartz + muscovite + kyanite + magnetite	
AM14	Quartz-kyanite schist	Quartz + muscovite + hematite	
AM15	Quartz-kyanite schist	Quartz + kyanite + muscovite	Kaolinite

Table 3. Major elements composition of rocks around Kuta

Samples															
	AM01	AM02	AM03	AM04	AM05	AM06	AM07	AM08	AM09	AM10	AM11	AM12	AM13	AM14	AM15
Major oxides wt %															
SiO ₂	90.01	94.80	54.80	52.40	60.80	47.00	86.60	84.20	27.52	28.34	94.60	55.40	72.00	91.70	66.60
Al ₂ O ₃	5.70	0.18	26.70	29.60	24.60	34.90	5.08	7.64	19.05	6.13	0.10	19.60	12.89	0.74	10.08
P ₂ O ₅	0.002	ND	ND	ND	ND	0.001	ND	0.001	0.32	0.73	ND	0.006	0.003	ND	0.003
Na ₂ O	1.00	ND	2.00	0.64	ND	1.51	2.00	ND	0.24	0.04	ND	0.84	2.03	0.04	1.22
K ₂ O	1.40	ND	1.80	0.083	ND	1.07	0.09	ND	0.46	0.44	0.24	0.082	3.60	2.01	0.088
CaO	0.69	0.063	0.49	0.13	0.048	0.84	0.26	0.19	0.09	0.17	0.12	0.16	0.54	0.02	0.20
MgO	0.008	ND	0.007	ND	ND	0.02	ND	ND	0.19	1.20	ND	ND	ND	ND	0.09
TiO ₂	2.01	2.90	ND	2.36	0.88	1.93	2.12	1.92	1.54	1.03	1.12	2.46	3.51	1.25	3.12
Fe ₂ O ₃	1.88	1.21	3.88	2.61	0.21	1.11	5.36	5.86	47.08	59.10	3.27	2.81	2.71	2.81	4.36
MnO	0.77	ND	ND	ND	0.01	0.083	0.06	0.002	1.19	2.03	0.061	0.53	0.001	0.005	0.05
LOI	1.02	0.74	13.02	12.00	13.00	11.20	1.42	1.20	0.59	2.49	0.42	15.00	2.80	1.24	10.42
Total	104.49	99.89	102.70	99.82	99.55	99.66	102.99	101.01	98.27	101.26	99.93	96.73	100.08	99.82	96.23

AM03, AM04, AM05, AM06, AM12= Mica schist

AM01, AM02, AM11= Quartzite

AM07, AM08, AM13, AM14, AM15=Quartz-kyanite schist

AM09, AM10=Banded Iron Formation (BIF)

ND=Not Determined

Table 4. Trace elements composition of rocks around Kuta

	Samples														
	AM01	AM02	AM03	AM04	AM05	AM06	AM07	AM08	AM09	AM10	AM11	AM12	AM13	AM14	AM15
	Trace elements (ppm)														
V	950	130	960	860	420	550	98	1000	315	311.04	1100	520	190	90	170
Cr	1200	1460	190	410	210	150	44	260	375	476.22	530	300	100	240	210
Ni	60	53.3	2.91	0.009	1.24	ND	ND	0.007	578.12	385.13	55.01	0.002	0.24	ND	0.19
Co	ND	ND	0.005	0.002	0.12	0.003	0.001	0.003	456	2997	ND	ND	0.15	ND	0.08
Rb	1230	38	100	38	45.02	72.01	120	98	15.23	32.41	45	51	140	0.002	39
Sr	2100	880	2200	ND	7.60	620	ND	ND	32.01	87	240	420	2750	0.032	210
Os	24	45	ND	ND	10	ND	ND	ND	ND	ND	ND	ND	10	2	ND
Ir	100	200	100	450	14	ND	3.20	20	ND	ND	ND	11	20	22	22
Cu	660	340	210	210	140	270	340	300	302	234.10	220	310	430	180	260
Pb	110	250	260	ND	6	430	46	390	421.40	538	230	130	20	10	110
Ag	ND	ND	ND	ND	ND	ND	ND	ND	ND	ND	ND	ND	ND	ND	ND
As	ND	ND	ND	ND	ND	ND	ND	ND	21.33	24.02	ND	31	10	5	14
Zn	33	ND	130	ND	ND	84	ND	ND	763	402	ND	34	ND	ND	38
Bi	33	ND	ND	3	ND	ND	ND	18	29	33	ND	22	ND	ND	32
Au	2	3	15	ND	6	ND	ND	ND	ND	ND	10	ND	3	ND	3
Ba	788	2700	1600	2900	ND	1300	ND	100	1048	997.21	500	600	ND	ND	200
Zr	1100	1100	450	1110	39	1100	920	760	103	107	490	600	1300	510	300
Ga	84	14	9.70	3	2	100	6	8	ND	ND	11	120	34	100	24
Y	31	ND	ND	ND	ND	120	ND	ND	ND	ND	ND	105	ND	ND	54
Ce	320	ND	1000	ND	ND	ND	ND	ND	ND	ND	ND	86	30	120	120
Ge	24	16	ND	21	ND	ND	ND	ND	ND	ND	9.40	19	ND	ND	28

AM03, AM04, AM05, AM06, AM12= Mica schist
 AM01, AM02, AM11= Quartzite
 AM07, AM08, AM13, AM14, AM15=Quartz-kyanite schist
 AM09, AM10=Banded Iron Formation (BIF)
 ND=Not Determined

Average CaO, MnO, and MgO, values are generally less than 0.85 wt% except for the BIF (with a mean MnO value of 1.61 wt%). The moderately rich manganese concentration of the BIF is contrary to the manganese concentration recorded by Bolarinwa [14] for the BIF of Ganfelum area northeastern Nigeria, Muro BIF central Nigeria by Adekoya et al. [16], and the iron ore occurrence near Kakun Kabba Nigeria [Abhulimen, 1986 unpublished] whose manganese concentrations are very low. This is also in disagreement with [15] who stated that Nigeria BIFs are characterized by enrichment with manganese. The increase in Fe₂O₃ with a decrease in Al₂O₃ may indicate replacement of precursor silica with goethite, which later dehydrated to hematite [14]. This is also similar to the observation of Mucke and Neumann [17] on the BIF of Itakpe area. Al₂O₃ increases with increase in TiO₂ may indicate different genetic source for the TiO₂ and Fe₂O₃ in the BIF samples [14].

Mean K₂O content is highest in the quartz-kyanite schist with the BIF's having the lowest value of 0.45 wt %. Average Na₂O is generally low, but the highest mean value of 1.32 wt% exists in the quartz-kyanite schist, while the least average value is noted in the BIF. Mean TiO₂ is very high in all the rock samples with the highest average value of 2.38 wt% in quartz-kyanite schist.

The enrichment of TiO₂ in the rock samples might due to replacement of Si with Ti or its mobility; and this is also indicated by the presence of rutile in the rock samples. It is also noted that most metasediments in Nigeria are very poor in TiO₂ which may indicate absence of Ti during geochemical mobility or metasomatic replacement of Si with Ti [6]. However, the concentrated value of P₂O₅ recorded for the BIF's ranged between 0.32-0.73 wt % averaging 0.53 wt % suggest an oxide facies type for the BIF [14].

In terms of trace elements content (Table 4), the schistose rocks (mica schist, quartz-kyanite schist, and quartzite) have abundance concentrations in the following trace elements when compared with the average composition of Post-Archean Australia Shale (PAAS) [18] and North American Shale (NASC) [19] with V ranged between (309.6-726.67 ppm), Sr (592.01-2200 ppm), Cu (228-406.67 ppm), Rb (61-437 ppm), Ba (150-1600 ppm), Zr (659-896.67 ppm), Y (31-112.5 ppm), Ce (135-543 ppm) with the exception of Ni (0.15-56.10 ppm), As (14.50-31

ppm), Co (0.03-0.06 ppm), and Zn (33-82.67 ppm) which have low concentration. The high abundance suggests the generation of the schistose rocks in the arc setting [20].

Trace elements concentration for the BIF reveal anomalous concentrations for some of the elements which include high contents of V (311-315 ppm) and Cr (375-476.22 ppm) when compared to other Precambrian BIFs in Nigeria, such as Banded Iron Formation of Northern part of Wonaka schist belt [Abdullahi, 2014 unpublished]; BIF of the Ganfelum area Northeastern Nigeria [14]; Maru BIF north-western Nigeria [21]; and Muro BIF Central Nigeria [16]. Ni (385.13-578.12 ppm) with a mean value of 481.63 ppm is high and similar to BIF of northern part of Wonaka schist belt [Abdullahi, 2014 unpublished]; Co (456-2997 ppm) is very high. Rb (15.23-32.41 ppm) is very low, Sr (32.01-87 ppm), Cu (234.10-302 ppm) is high, Cr (375-476.22 ppm) is slightly similar to those of BIF of northern part of Wonaka schist belt, and that of iron ore occurrence near Kakun Kabba [Abhulimen, 1986 unpublished]. Ba (997.21-1048 ppm) is also very high.

3.3 Discussion

A plot of Na₂O/Al₂O₃ against K₂O/Al₂O₃ [22] shows that the rock samples plot within the inference field of sedimentary/metasedimentary rocks as distinct from igneous field (Fig. 14).

This is also an indication that the rocks exhibit similar protolithic origin with other metasediments such as that of Okemesi schistose rocks [10], Wonaka schists belt (Abdullah, 2014 unpublished), [Taiwo, 1998 unpublished], Ilesha metasediments [23], Birnin Gwari schist [Ajibade, 1980 unpublished], and Burum-Takakafia mica schists [Ako, 2006 unpublished].

It was further deduced from the plot of Na₂O against K₂O [24] that the sediments (now metamorphosed) were derived from a mixed greywacke and arkosic rocks (Fig. 15). However the mica schist is constrained to the field of greywacke (Fig. 15); the quartz-kyanite schist shows heterogeneous or mixed protolith of greywacke and arkosic nature; and the quartzite have predominantly arkosic derivatives. The Kwakati schist [Taiwo, 1998 unpublished], and Burum-Takalafia schists [Ako, 2006 unpublished] show similar trend with that of the mica schist in the study area for their greywacke sediments type, while the quartz-kyanite schist is more similar to Okemesi schistose rocks [10], Lafiagi

and Osi quartz-mica-sillimanite schist [6], and Igarra quartz mica schist [25] for their arkosic sediments rich nature prior metamorphism.

In the plot of $\text{SiO}_2/\text{Al}_2\text{O}_3$ versus $\text{K}_2\text{O}/\text{Na}_2\text{O}$ (Fig. 18), the arc related nature of the schistose samples is revealed, since they plotted in the field of arc setting, basaltic and andesitic detritus to depict the arc related nature of the sediments prior metamorphism. This indicates similar tectonic settings with that of Okemesi schistose rocks [10].

AFM plot [26] Fig. 16 has shown that the rocks samples is tholeiitic in nature; and this is in agreement with [2] and [20] which emphasized that some schist belts in Nigeria include oceanic materials with tholeiitic affinities, indicating arc related nature of the metasedimentary rocks. Significant amount of Cr in the rock samples

indicate the presence of mafic constituents in the original sediments [11]. The mica schist is moderately matured metapelitic rock with tholeiitic affinity suggested to have derived from basaltic and andesitic detritus; the quartzite is meta-arkosic rock with tholeiitic affinity; the quartz-kyanite schist is moderately matured with a hybrid of meta-arkosic and metapelitic origin.

Fig. 17 revealed the peraluminous nature of the rocks samples as indicated on the plot of $\text{Al}_2\text{O}_3/(\text{Na}_2\text{O} + \text{K}_2\text{O})$ versus $\text{Al}_2\text{O}_3/(\text{CaO} + \text{Na}_2\text{O} + \text{K}_2\text{O})$ [after 23]. Presence of detrital topaz derived from the clay sediments is likely the cause of enhancement of Al and high value of loss of ignition in the geochemical results of some of the schist samples. This shows that topaz was an accessory mineral in the pre-existing rock from which the sediment (now metamorphosed) was sourced [10].

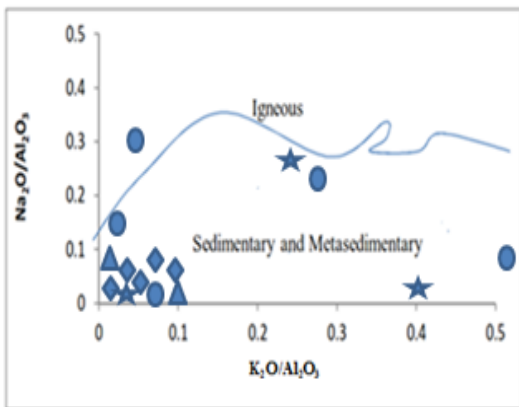


Fig. 14. $\text{Na}_2\text{O}/\text{Al}_2\text{O}_3$ vs. $\text{K}_2\text{O}/\text{Al}_2\text{O}_3$ plot for rocks around Kuta [22]

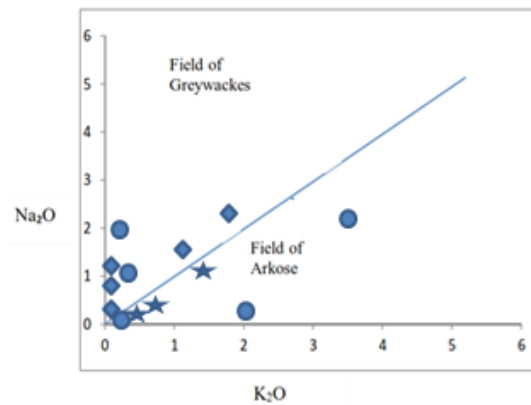


Fig. 15. Na_2O against K_2O plots for rocks around Kuta [24]

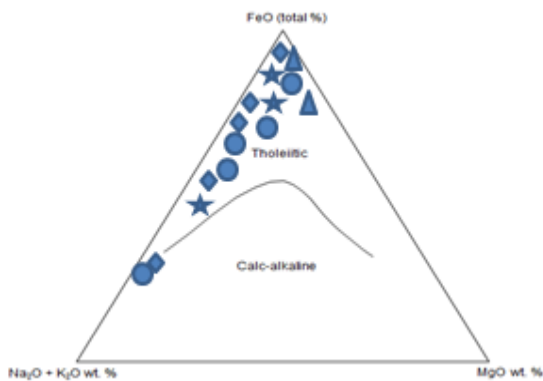


Fig. 16. AFM plot for rocks around Kuta [26]

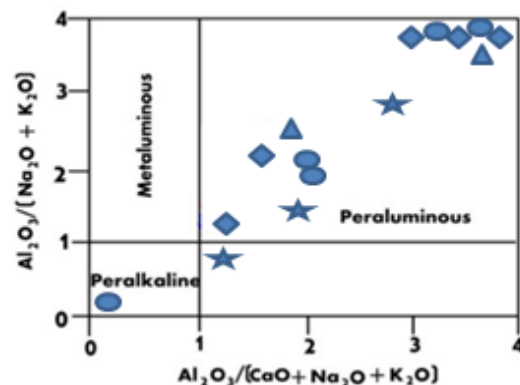


Fig. 17. $\text{Al}_2\text{O}_3/(\text{Na}_2\text{O} + \text{K}_2\text{O})$ Vs. $\text{Al}_2\text{O}_3/(\text{CaO} + \text{Na}_2\text{O} + \text{K}_2\text{O})$ molecular plot for rocks around Kuta [after 28]

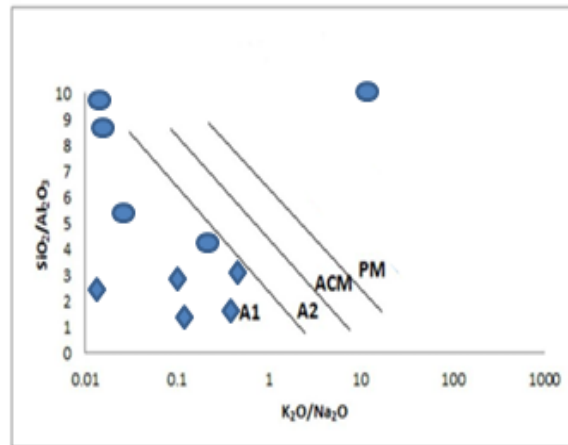


Fig. 18. $\text{SiO}_2/\text{Al}_2\text{O}_3$ Vs. $\text{K}_2\text{O}/\text{Na}_2\text{O}$ plot for schistose rocks around Kuta [20] ACM, active continental margin; PM, passive margin; A2, evolved arc setting, felsic-plutonic detritus; A1, arc setting, basaltic and andesitic detritus

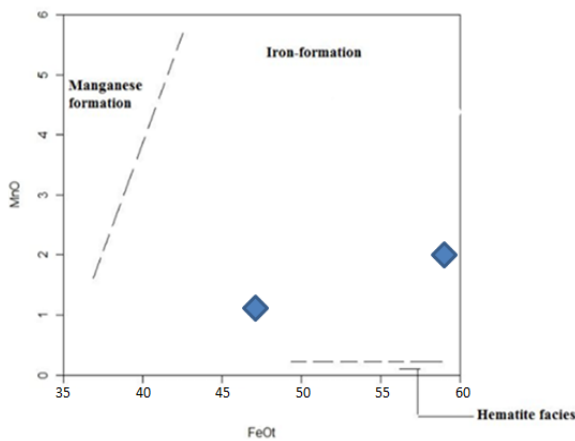


Fig. 19. MnO against FeO (tot) diagram (wt %) for BIF around Kuta [16]

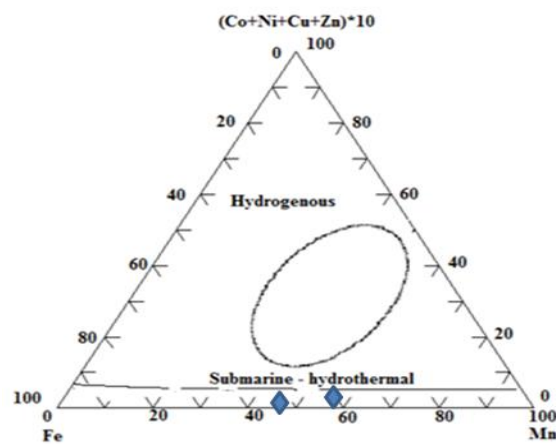


Fig. 20. Fe-Mn-(Co+Ni+Cu+Zn)*10 diagram for BIF around Kuta [27]

- ◆ Mica schist
- ★ Quartzite
- Quartz-kyanite schist
- ▲ Banded Iron Formation (BIF), the shapes above are applicable for Fig. 14-18

In the plot of MnO-FeOtot discrimination diagram [16] for the BIF in the study area (Fig. 19), shows that the BIF contains low to moderately rich manganese and high iron concentrations. The moderately rich manganese concentration of the BIF is slightly in contrary with the BIF of Gafelum area northeastern Nigeria [14], Muro BIF central Nigeria [16], and the iron ore occurrence near Kakun Kabba Nigeria [Abhulimen, 1986 unpublished] whose

manganese concentrations are very low. This is also in disagreement with [16] that Nigeria BIFs are characterized by enrichment of manganese. The ternary plot of Fe-Mn-(Co+Ni+Cu+Zn)*10 diagram [27] shows that the BIF from the study area are submarine-hydrothermal source (Fig. 20). Trace element data enrichment in Ni, Co, and V also indicates the dual provenance, terrigenous and submarine hydrothermal with magnetite silicate facies types for the BIF.

Table 5. Comparison of rock samples from the study area with industrial specification of refractory kyanite

Major Oxides	BSI (%) [29]	ASTM (%) [30]	BIS (%) [31]	Kuta mica schist	Kuta Quartzite	Kuta quartz-kyanite schist	Kuta BIF
SiO ₂	42.00 max	39.01 max	39.00 max	54.08	93.14	80.22	27.93
Al ₂ O ₃	56.00 min	56.50 min	58.0 min	27.08	1.99	7.23	12.59
Fe ₂ O ₃	1.00 max	0.80 max	2.0 max	2.55	2.12	4.22	53.09
TiO ₂	-	0.18 max	2.0 max	1.91	2.01	2.38	1.29
CaO	-	0.09 max	-	0.33	0.29	0.24	0.45
MgO	-	0.002 max	-	0.01	0.008	0.09	0.70
Na ₂ O	-	0.01 max	-	1.25	1.00	1.32	0.14
K ₂ O	-	0.02 max	-	0.76	0.82	1.45	0.45
P ₂ O ₅	0.1 max	-	-	-	0.002	0.002	0.53
LOI	-	-	-	12.84	0.73	3.42	1.54
Fe ₂ O ₃ + TiO ₂	-	-	2.5 max	4.46	4.13	6.60	54.38
Na ₂ O + K ₂ O	-	-	0.5 max	2.01	1.82	2.77	0.59
Fe ₂ O ₃ + TiO ₂ + CaO + MgO + Alkalis	-	-	3.5 max				

(Table 5) is the comparison of the kyanite-bearing rocks in the study area with some industrial specifications of refractory kyanite grade.

4. CONCLUSION

The present detailed evaluation (via petrographic, mineralogy, and geochemistry) have confirmed the occurrence of kyanite mineralization in three (3) lithological units (mica schist, quartzite, and quartz-kyanite schist) around Kuta north central, Nigeria.

The petrology and geochemistry of the rocks in Kuta area indicate sedimentary protolith for the four (4) lithological units, the mica schist; quartzite; quartz-kyanite schist; and BIF.

Based on the mean percentage of kyanite composition and the results of the major defining chemical elements such as alumina and silica mean percentage values, the kyanite cannot be used as an important industrial raw material input for the production of monolithic refractory which find uses in furnaces (for glass, melting, non-ferrous metals, ceramics, and cement kilns) and in foundry. These chemical properties do not meet the standard requirements of kyanite for industrial use.

The chemical composition of commercial refractory grade raw materials which are marketable all over the world is characterised by high Al_2O_3 and low contents of fluxing oxides, that is generally <1% Fe_2O_3 , <2% TiO_2 , <0.5% Na_2O+K_2O and <0.5% $MgO+CaO$ for which is an exception for kyanite bearing rocks around Kuta north central, Nigeria.

The mineralogical analysis (via XRD) and modal analysis during petrographic studies show that the percentage composition of kyanite in the kyanite bearing rocks around Kuta north central Nigeria is greatly below the acceptable limit when compare to other economic kyanite deposits around the world.

COMPETING INTERESTS

Authors have declared that no competing interests exist.

REFERENCES

1. Truswell JF, Cope RN. The geology of parts of Niger and Zaria Provinces,

Northern Nigeria. Geological Survey of Nigeria. 1963;29:1-104.

2. Dada SS. Proterozoic evolution of Nigeria. In: Oshin O. (ed) The Basement Complex of Nigeria and its Mineral Resources Petroc. Services Ltd. Ibadan, Nigeria. 2006;29-45.

3. Rahaman MA. Recent advances in the study of the basement complex of Nigeria. Abstract, 1st Symposium on the Precambrian Geology of Nigeria; 1981.

4. Obiora SC. Field descriptions of hard rocks with examples from the Nigerian Basement Complex (1st Edition). Snap Press (Nig.) Ltd. Enugu. 2005;14.

5. Van Noy RM. Kyanite resources in North-western United State Report of Investigation 7426, US Bureau of Mines. 1970;81-82.

6. Adedoyin AD, Adekeye JID, Ojo OJ. Geochemical composition and petrogenesis of schists and amphibolites of parts of sheets 203 (Lafiagi) SW and 224 (Osi) NW, Southwestern Nigeria. ILJS-14-013. 2014;1(1):1-17.

7. Janousˇek V, Finger F, Roberts M, Fry´da J, Pin C, Dolejsˇ D. deciphering the petrogenesis of deeply buried granites: whole-rock geochemical constraints on the origin of largely undepleted felsic granulites from the Moldanubian Zone of the Bohemian Massif. Transactions of the Royal Society of Edinburgh: Earth Sciences. 2004;95:141-159.

8. Tanner AO. Kyanite and related minerals (Advanced Released): U.S. Geological Survey 2012 Minerals Yearbook, August; 2013.

9. Omang BO, Alabi AA. Geochemistry and mineralogical evaluation of quartzite bearing Kyanite in Kuta, Northwestern Nigeria. Ethiopian Journal of Environmental Studies and Management. 2001;4(3).

10. Okunlola OA, Okorojafor RE. Geochemical and petrogenetic features of the schistose rocks of Okemesi fold belt, Southwestern Nigeria. Materials and Geoenvironment. 2009;56:148-162.

11. Ayodele SO. Litho-geochemical and petrogenetic characteristics of somemassive and schistose quartzites in Ekiti State, Southwestern Nigeria. 2014; Ijsit3(1):013-040.

12. Cox R, Lowe DR. Controls on sediment composition on a regional scale.

- Conceptual view; J Sed. Res. A. 1995;65:1–12.
13. Adekoya LA. The Nigerian schist belts: Age, and depositional environment implications from associated banded iron formations. *Journal of Mining and Geology*. 1996;32:35-46.
 14. Bolarinwa TA. Petrography and geochemistry of the banded iron formation of the Gangfelum area, Northeastern Nigeria. *Earth Science Research*. Publ. by Canadian Center of Science and Education. 2018;7(1);2018.
 15. Mucke, A. The Nigerian manganese-rich iron-formations and their host rocks from sedimentation to metamorphism. *African Journal. Earth Sci.* 2005;41:407-436.
 16. Adekoya JA, Okonkwo CT, Adepoju MO. Geochemistry of Muro Banded Iron-Formation, Central Nigeria. *International Journal of Geosciences*, 3, 1074-1083. African Geology, University of Ibadan press. 2012;67-99.
 17. Mucke A, Neumann U. The genesis of the banded iron ore deposits of Itakpe area, Kwara State, Nigeria. *Fortachritte der Mineralogie*. 1986;64:187-204.
 18. Taylor SR, McLennan SM. The continental crust: Its composition and evolution. Oxford, Blackwell Scientific Publishing. 1985;312.
 19. Gromet LP, Dymek RF, Haskin LA, Korotev RL. The "North American shale composite": Its compilation, major and trace element characteristics *Geochimica et Cosmochimica Acta*. 1984;48: 2469-2482.
 20. Roser BP, Korsch RJ. Determination of tectonic setting of sandstone-mudstone suites using SiO₂ content and K₂O/ Na₂O ratio. *The Journal of Geology*. 1986; 94(5):635–650.
 21. Adekoya JA. The geology and geochemistry of the Maru Banded Iron Formation, Northwestern Nigeria. *Journal of African Earth Sciences*. 1998;27(2):241-257.
 22. Garrels RM, MacKenzie FT. Evolution of sedimentary rocks. W.W. Norton and Company, New York. 1971;394.
 23. Elueze AA. Dynamic metamorphism and oxidation of amphibolites of Tegna Area, North-western Nigeria. *Precambrian Research*. 1981;14(3):379-388.
 24. Pettijohn FJ. Sedimentary rocks, New York, Harper and Brothers. 2nd edition. 1975;718.
 25. Okeke PO, Meju MA. Chemical evidence for the sedimentary origin of Igarra Supracrustal rocks S.W. Nigeria. *Jour. Min. and Geol.* 1985;22(1 and 2):97–104.
 26. Irvine TN, Baragar WRA. A guide to the chemical classification of the common volcanic rocks: *Canadian Journal of Earth Sciences*. 1971;8:523-548.
 27. Bonatti E, Kraemer T, Rydell H. Classification and genesis of submarine iron manganese deposits In Horn DR. (E.d.), Conference of Ferromanganese Deposit on the Ocean Floor. Harriman New York, Anden House. 1972;149-166.
 28. Maniar PD, Piccoli PM. Tectonic discrimination of granitoids. *Geol. Soc. Amer. Bull.* 1989;101:635-643. Available: [https://doi.org/10.1130/00167606\(1989\)101<0635:TDOG>2.3.CO;2](https://doi.org/10.1130/00167606(1989)101<0635:TDOG>2.3.CO;2).
 29. British Standard Institution (BSI) 1335:1979: Method for direct determination of alumina in refractory materials (first revision); 1979.
 30. American Society for Testing and Materials (ASTM); 2005. Available:<http://www.astm.org>
 31. Bureau of India Standard (BIS). Non-metallic and Industrial Mineral Group; 1985. Available:http://www.geologydata.info/non_metallic

© 2018 Muhammed et al.; This is an Open Access article distributed under the terms of the Creative Commons Attribution License (<http://creativecommons.org/licenses/by/4.0>), which permits unrestricted use, distribution, and reproduction in any medium, provided the original work is properly cited.

Peer-review history:

The peer review history for this paper can be accessed here:
<http://www.sciencedomain.org/review-history/26675>